DYNAMIC MEASUREMENT OF SURFACE CHARGE

Y L Sam, P L Lewin, A E Davies, J S Wilkinson, S J Sutton[+] and S G Swingler[+]

University of Southampton, UK

[+]The National Grid Company plc, UK

INTRODUCTION

This paper describes the development of a system capable of monitoring the dynamic movement of surface charge on insulating materials. High electrical stress can be generated at the edges of an interface between a conductor and solid insulation by the existence of a non-uniform field. This may cause local sparking and corona along the surface of the insulation. The presence of surface discharge activity is a significant problem for organic insulators. Any discharge can cause a slow deterioration of the insulator surface in the long term through three mechanisms: Slow erosion by ionic bombardment of ions in the sparks, chemical degradation and carbonisation of the surface material. Conducting deposits are formed on the surface and this will influence the electrical characteristics of the insulator. The development of a suitable method to monitor surface discharge behaviour of high voltage (hv) insulating materials is therefore of particular interest.

Established methods of measuring surface charge include the dust figure technique (1,2) and the electrostatic scanning probe method (3). The dust figure technique involves spraying a charged powder onto the surface of the material in order to observe the charge pattern. The dust used is a mixture of positively charged red-coloured lead oxide and negatively charged yellow-white sulphur. Although inexpensive and simple to perform, the method does not quantify the amount of charge or allow dynamic movement of charge to be visualised.

Electrostatic scanning probes often have low spatial and charge resolution, are relatively slow and may influence the electric field around the measurement point. The area of the surface charge to be measured influences the probe output and the thickness of the dielectric material can influence the accuracy of the measurement. As the sample thickness is increased, the potential distribution across it becomes less uniform. The coexistence of positive and negative charge on the same surface can cause measurement errors of up to 15% (3).

The measurement system described in this paper is based on the use of a birefringent crystal as the sensing element. The method utilises the electro-optic effect (Pockels effect) of the crystal in order to detect the local electric field (4). The test material is bonded to the backface of the crystal and any surface charge upon it will alter the local field within the crystal. The field will affect the polarisation of light passing through the crystal and the amount of reflected light for a given angle of polarisation can be easily measured. Determining the change in polarisation of the reflected light allows the local charge density to be calculated. Consequently, this method has significant advantages over existing methods as it enables the observation of dynamic of surface discharge behaviour and the charge density to be determined simultaneously.

POCKELS EFFECT

Crystals that lack a centre of symmetry such as Lithium Niobate ($LiNbO_3$) and Bismuth Silicate (BSO) exhibit the linear electro-optic effect or Pockels effect. This means that the refractive index, n, of some or all of the crystal axes is linearly dependent on an applied electrical stress. In this application, any induced birefringence is proportional to the applied electric field. The major industrial application for these crystals is light modulation, however they can also be used as described here to measure an applied stress.

There are two common cell configurations of a Pockels device when used to measure electric stress. In the transverse mode, the electric field is perpendicular to the direction of light propagation. This mode is commonly used for light modulation (5) and electric field measurement (6). In the longitudinal mode the electric field is parallel to the direction of light propagation. The longitudinal mode can be used to measure surface charge (Figure 1). BSO is uniaxial and free of natural birefringence in the absence of an electric field and consequently is ideal for this application.

With reference to Figure 1, the crystal is arranged so that two of its axes are at an angle of 45° to the incident polarised light. If an electric stress is applied in the direction of the third crystal axis and parallel to the direction of light propagation then the field will induce fast and slow axes in the plane normal to itself. The linearly polarised light will be transformed on passing through the crystal to elliptically polarised light; further increasing the field will result in circular polarisation. The difference in refractive index between the fast and slow axes is proportional to the applied electric field. The phase retardation, θ, of the

Dielectric Materials, Measurements and Applications
Conference Publication No. 473, © IEE 2000

light due to the induced fast and slow axes from an applied electric stress of E Vm^{-1} is:

$$\theta = \frac{2\pi}{\lambda} n_0^3 r_{41} E d \qquad (1)$$

Where λ is the wavelength of the incident polarised light, n_0 is the refractive index for normal light (2.54 for BSO), r_{41} is the relevant electro-optic coefficient (5.10^{-12} mV^{-1}) and d is the thickness of the crystal

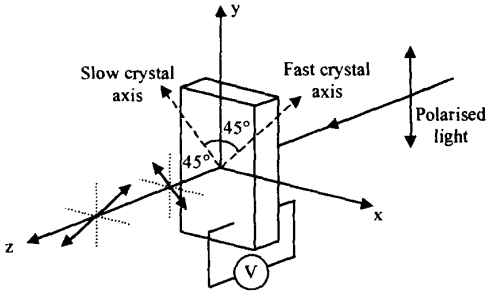

Figure 1: Pockels crystal arranged in longitudinal mode

PRACTICAL IMPLEMENTATION

A HeNe laser source (Figure 2) provides polarised light of wavelength 632.8nm that is passed through a beam expander and a polarising beam splitter (pbs). A 1/8 waveplate is placed between the pbs and the Pockels cell. The waveplate acts to bias the transmission of the system to half its maximum intensity. The orientation of the cell is adjustable and the crystal axes are arranged with respect to the polarisation of the incident radiation as shown in Figure 1. The crystal used in this experiment is BSO (15mm square, 0.5mm thick) coated with a thin gold film (≈30nm) on its front face. The gold acts as a transparent electrode and is grounded. In order to generate surface charge a needle tip is in contact with the sample surface on the other side of the crystal. The needle is connected to an AC generator that can supply up to 5kV at 50 Hz. The needle has a 5μm radius, which is small enough to generate high electric fields and initiate electrical discharge.

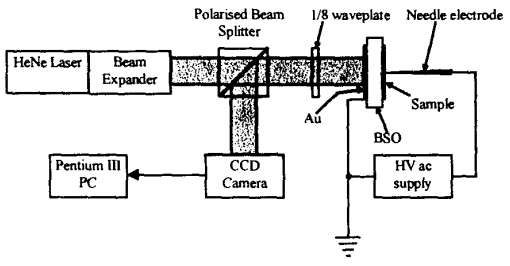

Figure 2: Practical implementation

Light entering the BSO crystal is reflected from the interface between the sample and the backface of the crystal. Consequently, the light will travel through the crystal twice. From Equation 1 this will double the amount of phase retardation for a given surface charge and therefore double the sensitivity of the measurement. The reflected light passes through the transparent electrode and is returned to the pbs. The pbs directs the components of the reflected light that have phase retardation due to surface charge towards the CCD camera. The CCD camera detects the incident light intensity at a maximum rate of 1000 frames per second and quantifies it into 255 levels. The CCD camera has sufficient memory to store successive frames of images and these can be transferred to a PC for post-processing.

Determination of phase retardation

BSO has no natural birefringence and therefore both polarities of charge will have an identical effect on the light intensity incident on the CCD if the crystal is unbiased. In order to distinguish between positive and negative charge the 1/8 waveplate is used to bias the transmission of the Pockels cell to half of the incident light intensity (Figure 3). Once the stress to be measured is applied to the sample, a positive charge will increase light intensity whereas a negative charge will decrease the light intensity.

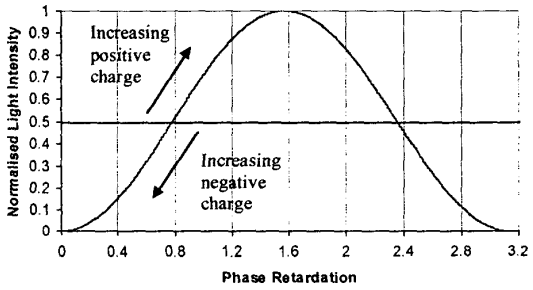

Figure 3: Biased light intensity using a 1/8 waveplate

The general equation for light intensity, I, due to a phase retardation, θ, measured using the CCD camera is given as:

$$I_{(x,y)} = I_{0(x,y)} \sin^2\left(\theta_{(x,y)}\right) \qquad (2)$$

Where I_0 is the maximum light intensity of the polarised light and the x,y coordinates relate to a single pixel of the CCD array. If a 1/8 waveplate is inserted between the pbs and the Pockels cell then the measured light intensity is given as:

$$I_{(x,y)} = I_{0(x,y)} \sin^2\left(\frac{\pi}{4} + \theta_{(x,y)}\right) \qquad (3)$$

Assuming that there is no surface charge present on the sample prior to application of the high voltage, the

initial observed light intensity, I_I, will be:

$$I_{I(x,y)} = I_{0(x,y)} \sin^2\left(\frac{\pi}{4}\right) = \frac{I_{0(x,y)}}{2} \quad (4)$$

Once the voltage is applied the camera records the change in light intensity at 1ms intervals. From Equations 3 and 4 the measured light intensity due to surface charge, I_Q, is:

$$I_{Q(x,y)} = 2I_{I(x,y)} \sin^2\left(\frac{\pi}{4} + \theta_{(x,y)}\right) = I_{I(x,y)}\left[1 - \cos\left(\frac{\pi}{2} + 2\theta_{(x,y)}\right)\right] \quad (5)$$

Expanding the cosine term gives:

$$I_{Q(x,y)} = I_{I(x,y)}\left[1 + \sin\left(2\theta_{(x,y)}\right)\right] \quad (6)$$

Hence the phase retardation is:

$$\theta_{(x,y)} = \frac{1}{2}\sin^{-1}\left(\frac{I_{Q(x,y)} - I_{I(x,y)}}{I_{I(x,y)}}\right) \quad (7)$$

The surface charge density, σ, is related to the electric field by

$$\sigma_{(x,y)} = \varepsilon_0 \varepsilon_r E_{(x,y)} \quad (8)$$

Where ε_0 is the permittivity of free space ($8.85.10^{-12}$ Fm^{-1}) and ε_r is the relative permittivity of BSO (56). Therefore from Equations 1 and 7 the surface charge density can be defined as:

$$\sigma_{(x,y)} = \frac{\varepsilon_0 \varepsilon_r \lambda}{4\pi n_0^3 r_{41} d} \sin^{-1}\left(\frac{I_{Q(x,y)} - I_{I(x,y)}}{I_{I(x,y)}}\right) \quad \left(Cm^{-2}\right) (9)$$

EXPERIMENTAL RESULTS

A 4kV 50Hz ac voltage was applied via a needle electrode to a Pockels cell that did not have a test sample bonded to its backface. The aim of the experiment was to validate the proposed method, ensuring that the system was capable of quantifying the amount of surface charge and observing its dynamic properties. An additional electronic circuit was developed to synchronise the camera framing rate with the applied ac waveform and ensure that the camera recorded the initial light intensity before the ac waveform was applied (Figure 4). A burst of two power cycles was generated resulting in forty frames of measurement data.

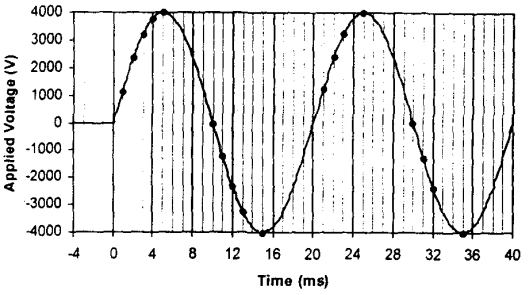

Figure 4: Applied voltage and CCD camera framing instants.

The captured frames of data were transferred to a PC for processing. After filtering to remove background noise, the measured light intensity at each pixel was used to determine its instantaneous surface charge. The obtained results for the framing instants detailed in Figure 4 are presented in Figures 5 to 8.

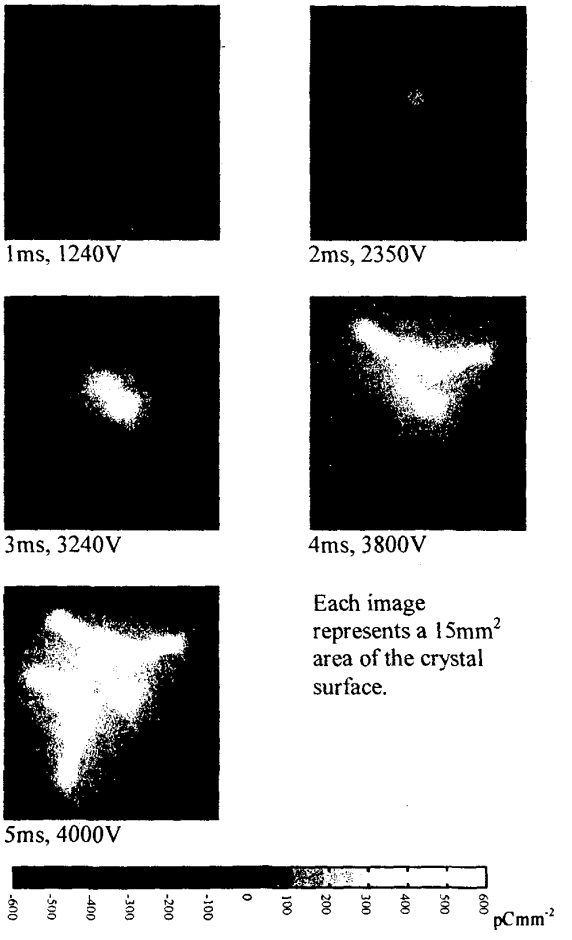

Figure 5: Charge distribution for the first positive half cycle (0-5ms)

No measurable surface charge is observed 1ms after the ac voltage is initially applied. After 2ms there is

positive charge deposited on the crystal surface near to the needle tip. Although initially circular in shape, the deposited charge does not increase uniformly across the crystal surface, as seen after 3ms. As the applied voltage continues to increase, more charge is deposited and positive streamers flow in a radial direction away from the needle tip. After 5ms the applied voltage is at its maximum and the positive streamers stop travelling away from the needle tip and are at their maximum length. During the following 5ms the applied voltage falls, the positive streamers remain on the surface of the crystal and there is virtually no movement of the observed charge. When the applied voltage passes through zero the positive charge on the surface near the needle tip is neutralised. Figure 6 shows the measurements of surface charge distribution during the first negative half cycle.

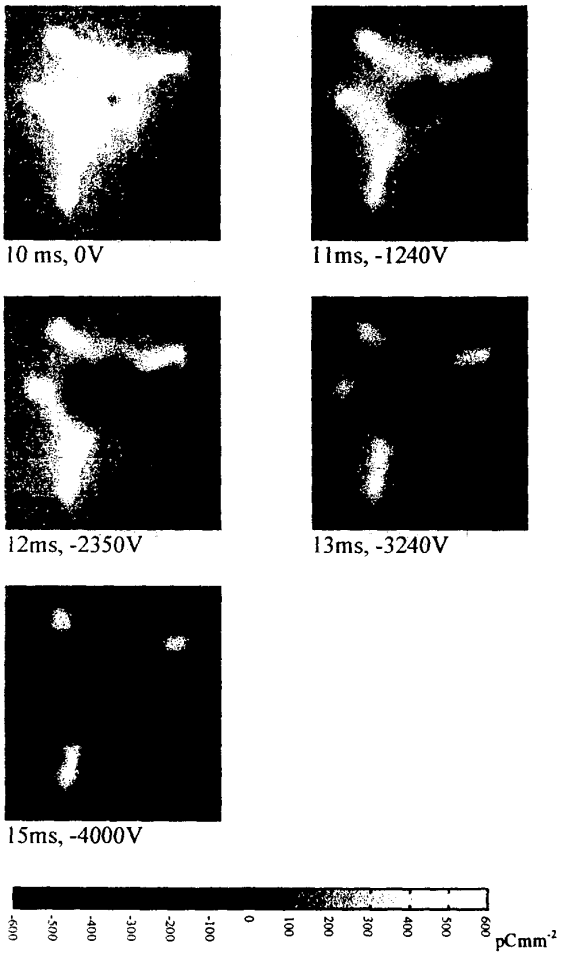

Figure 6: Charge distribution for the first negative half cycle (10-15ms)

As there is positive charge on the crystal, as soon as the applied voltage falls below zero negative charge is deposited. This is known as negative backdischarge (1,4). Approximately circular in distribution, the deposited charge is concentrated around the needle tip. As the applied voltage continues to decrease the negative charge density continues to increase and expand radially (Figure 6, 11 and 13 ms). The negative charge does not develop streamers and even when the applied voltage is –4kV the positive streamer tips have not been neutralised (Figure 6, 15ms) although the negative charge has expanded to its maximum density and radius. As with the first positive half cycle the surface charge pattern remains unaltered as the applied voltage increases towards zero volts.

At the start of the second cycle positive streamers are again formed (Figure 7). Due to positive backdischarge some positive charge is observed around the zero crossing point. The presence of the negative charge distorts the propagation of the positive streamers and they only develop within the negatively charged region (figure 7, 21-23ms). When the applied voltage is 4kV (25ms) the deposited positive charge appears to have neutralised all of the negative charge. The original streamer tips from the first positive half cycle can still be clearly observed and comparison with images for 23ms and 25ms reveals that an additional streamer has developed in the lower right hand quadrant of the image.

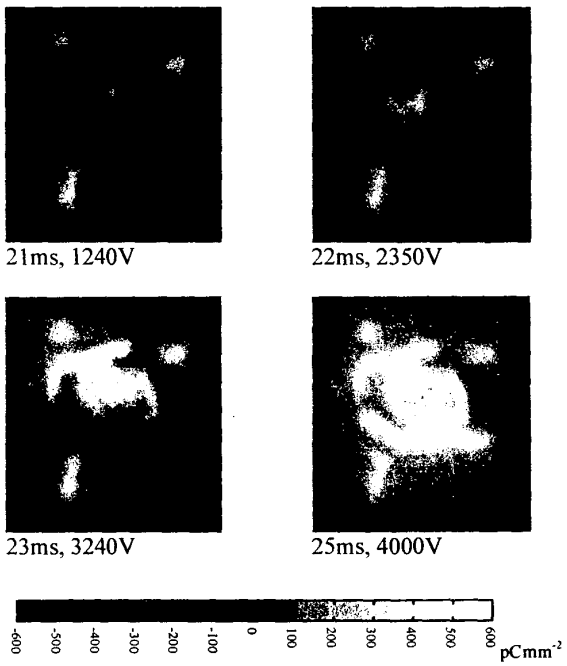

Figure 7: Charge distribution for the second positive half cycle (20-25ms)

As the voltage decreases toward zero there is no movement of surface charge. Around zero volts, negative charge is again observed (Figure 8); the distribution expands radially and increases in density as the applied voltage decreases. Again only the tips of

the positive streamers remain by the time that the applied voltage has reached –4kV (Figure 8, 35ms).

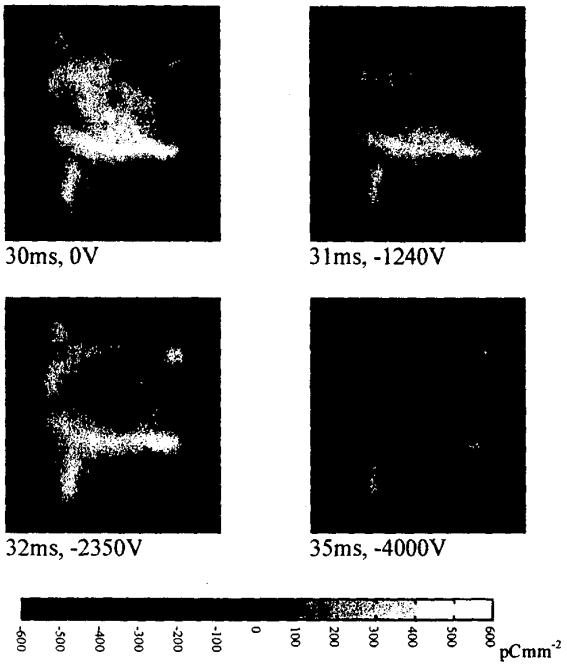

Figure 8: Charge distribution for the second negative half cycle

The positive streamer pattern that is observed during the second positive half cycle is very different to that observed during the first. This is due to the number of initially available free electrons around the needle electrode. During the first positive half cycle, free electrons are present in the surrounding air generated by either cosmic rays or electron detachment from negative ions. During the positive half cycle these electrons are attracted to the anode and leave low-mobility positive ions within the region. The number of the positive streamers depends upon the applied voltage and the number of initially free electrons. In the case of the second positive half cycle, electrons have been liberated from the needle electrode during the previous negative half cycle. As the applied voltage becomes positive for the second cycle, the positive streamers neutralise the electrons present around the needle tip.

Backdischarge occurs as the applied voltage approaches zero volts but before the zero crossing point is reached. In the case of negative backdischarge, as the positive electric field is applied to the needle the electrons move from the weak field region to high field region. These electrons accumulate around the needle tip and the electron density becomes high (1) achieving equilibrium with the needle tip. As the applied stress starts to decrease, the equilibrium is no longer maintained and the opposite charge strength becomes higher than the applied field. The field gradient between the positive and negative charge is high enough to cause the return flow of electrons and hence neutralise the centre part of the streamers as observed in Figure 6 (10ms) and Figure 8 (30ms). During the negative half cycle electrons are liberated from the needle tip and move uniformly from the high field region to the weak region leaving positive charge near the needle tip. As the applied negative field starts to decrease equilibrium is not maintained. The electric field due to positive charge around the needle tip is now higher than the needle tip itself causing positive streamers to burst out and neutralise the electrons present (Figure 7(21ms)).

CONCLUSIONS

A method of surface charge measurement has been developed utilising the Pockels effect. This has enabled the measurement of surface charge to be visualised and quantified simultaneously. The dynamic properties of an ac discharge have been observed and the feasibility of the experimental approach proven. Future developments will include improving the temporal and spatial resolution of the measurement as well as investigating the surface charge behaviour of polymeric insulation materials. It is envisaged that the technique will be adapted to allow the effect on surface charge behaviour due to environmental parameters such as local atmosphere, pressure and ambient temperature to be investigated.

ACKNOWLEDGEMENT

The support and permission to publish by The National Grid Company plc for this work is gratefully acknowledged.

REFERENCES

1. Y Murooka, S Koyama, 1973, J Appl Phys, 1576-1580

2. Y Murooka, S Koyama, 1979, J Appl Phys, 6200-6206

3. H Ootera, K Nakanishi, 1988, IEEE Trans on Power Delivery, 165-171

4. T Kawasaki, Y Arai, T Takada, 1991, Japanese Journal of Appl Phys, 1262-1265

5. K Hidaka, 1996, DEIS, 17-28

6. T Minemoto, K Okamoto, K Miyamoto, 1985, Applied Optics, 2055-2062